

## FMR study of agglomerated nanoparticles in a Fe<sub>3</sub>C/C system

N. GUSKOS<sup>1,2\*</sup>, J. TYPEK<sup>2</sup>, M. MARYNIAK<sup>2</sup>,  
U. NARKIEWICZ<sup>3</sup>, I. KUCHARIEWICZ<sup>3</sup>, R. WRÓBEL<sup>3</sup>

<sup>1</sup>Solid State Section, Department of Physics, University of Athens,  
Panepistimiopolis, 15 784 Zografos, Athens, Greece

<sup>2</sup>Institute of Physics, Szczecin University of Technology, al. Piastów 17, 70-310 Szczecin, Poland

<sup>3</sup>Institute of Chemical and Environment Engineering,  
Technical University of Szczecin, al. Piastów 17, 70-310 Szczecin, Poland

Three samples with various Fe<sub>3</sub>C/C ratios have been prepared by the carburisation of iron with ethylene or an ethylene–hydrogen mixture. Carburisation was controlled with thermogravimetry. After carburisation, the samples were characterized using XRD and scanning electron microscopy. XRD measurements have shown the presence of the Fe<sub>3</sub>C (cementite) phase only. The mean size of cementite crystallites estimated using Scherrer's equation was in the range of 40–46 nm. Ferromagnetic resonance (FMR) absorption signals were investigated at room temperature. In all samples an asymmetric, very broad, and intense FMR line shifted toward low magnetic field was recorded. The linewidth, intensity, and position of the resonance field depended strongly on carbon concentration. With increasing carbon concentration the linewidth and integrated intensities of the FMR spectra decreased, and the resonance line shifted towards higher magnetic fields. The separation of granules from each other by carbon could drastically influence the FMR absorption spectrum due to decreasing intergranular interaction with increasing carbon concentration.

Key words: *magnetic resonance; nanoparticle; cementite*

## 2. Introduction

Carbon–iron based nanoparticles are of growing interest due to their improved magnetic properties as well as their potential applications in catalysis, sensor techniques, and the potential reduction of costs required to produce bulk quantities of these products [1–5]. In particular, nanocomposites of iron carbides, such as the ce-

---

\*Corresponding author, e-mail: ngouskos@cc.uoa.gr

mentite phase ( $\text{Fe}_3\text{C}$ ), are further suited to diverse technological exploitation due to their enhanced mechanical properties [6] and importance in ferrous metallurgy [7]. Meanwhile,  $\text{Fe}_3\text{C}$  nanoparticles were found to be more resistant to oxidation than  $\alpha\text{-Fe}$  nanoparticles due to the formation of amorphous carbon layers on their surfaces [1, 2].

Ferromagnetic resonance (FMR) has been long exploited to measure the magnetocrystalline anisotropy of magnetite single crystals as a function of temperature [8], as well as the shift of the FMR spectra of polycrystalline  $\text{Fe}_3\text{O}_4$  as a function of oxidation below the Verwey transition [9], and to identify fine-grained iron and iron oxide precipitates in natural glasses [10–12] and coal minerals [13]. More recently, FMR has emerged as a powerful and sensitive method to characterize magnetic nanoparticles. It relies mainly on the averaging effect of superparamagnetism on the FMR spectra of an assembly of non-interacting single domain nanoparticles, characterized by an orientation distribution of local anisotropy axes [14–21]. Relatively narrow FMR lines have been commonly observed in the high temperature regime in either dilute suspensions of iron-based oxide nanoparticles in ferrofluids [14] or dispersed in glass [13] or polymer matrices [20]. A narrow resonance line is considered as a fingerprint of superparamagnetic resonance at high temperatures, where thermal fluctuations partially average orientation distributions of local anisotropy fields, which become important at lower temperatures and lead to resonance line shapes similar to the FMR of polycrystalline systems [14–16]. In the case of iron non-oxide systems (e.g.  $\alpha\text{-Fe}$  or  $\text{Fe}_3\text{C}$ ) with strong exchange interactions, a very intense broad resonance line is observed [17, 18]. The FMR spectrum of nanoparticle agglomerates of iron carbide in a carbon matrix strongly depends on the concentration of magnetic nanoparticles.

The aim of this work is to study the FMR spectra of three samples differing in their  $\text{Fe}_3\text{C}/\text{C}$  ratio. The separation of iron carbide granules by carbon could influence the FMR absorption spectrum through intergranular and intermolecular interactions that vary with carbon concentration.

## 2. Experimental

Three samples with various cementite to carbon ratios (sample I – 1:0, sample II – 1:1, and sample III – 1:3) have been prepared by the carburisation of nanocrystalline iron with an ethylene–hydrogen mixture (sample I) or with pure ethylene (samples II and III).

The fusion of magnetite with small amounts of promoter oxides ( $\text{Al}_2\text{O}_3$  and  $\text{CaO}$ ) has been used for obtaining nanocrystalline iron. The obtained material was crushed, sieved (to obtain the fraction 1.2–1.5 mm), and reduced under hydrogen. After reduction, the obtained pyrophoric sample was cooled to room temperature and passivated under nitrogen with traces of oxygen, in order to avoid dramatic oxidation in contact with air.

The chemical compositions of samples were determined using an inductively coupled plasma atomic emission spectroscopy (AES-ICP). Beside iron, the samples con-

tained about 3 wt. % of both  $\text{Al}_2\text{O}_3$  and  $\text{CaO}$ . The average size of iron crystallites, determined using X-ray diffraction (Philips X'Pert equipment,  $\text{CoK}_{\alpha 1}$  radiation) and calculated using Scherrer's equation, amounted to 17 nm. The specific surface area of the samples, determined by the thermal desorption of physisorbed nitrogen (ASAP 2010, Micromeritics), was  $22 \text{ m}^2/\text{g}$ .

The carburisation process was monitored using a thermogravimetric method. The grains of the sample (0.5 g) were placed as a single particle layer in a platinum basket hung in a thermobalance and changes in the mass of the sample were recorded. Before carburisation, the samples were reduced (in order to remove the passivation layer) at temperatures rising from 293 to 773 K under a hydrogen flow. After achieving the reduction process (when a constant mass of the sample was maintained), carburisation was started through the addition of ethylene to hydrogen (sample I) or through a replacement of hydrogen by ethylene (sample II and III). A gas flow of  $1.3 \text{ dm}^3 \cdot \text{g}^{-1} \cdot \text{min}^{-1}$  was applied at a constant temperature of 673 K. An increase in the mass of the sample during the process was recorded, and when a determined degree of carburisation was reached the process was stopped by rapidly cooling the sample in a nitrogen atmosphere. After carburisation the samples were characterised by XRD (Philips X'Pert equipment,  $\text{CoK}_{\alpha 1}$  radiation) and SEM (digital scanning electron microscope Zeiss LEO).

The FMR measurements were carried out at room temperature, using a Bruker 500 D spectrometer working in the X-band ( $\nu = 9.43 \text{ GHz}$ ) at a 100 kHz magnetic field modulation. The samples, each containing around 10 mg of the material, were placed into 4 mm diameter quartz tubes.

### 3. Results and discussion

The relative change of the mass of the samples during carburisation, expressed as the ratio of carbon to iron carbide mass, is presented in Figure 1. The first sample was carburised under an ethylene:hydrogen 1:3 mixture until the mass increase equivalent to the formation of iron carbide ( $\text{Fe}_3\text{C} - 0.072 \text{ g C/g Fe}$ ) was reached (TG 1). Then the ethylene/hydrogen mixture was replaced by nitrogen and the heating of the reactor was stopped. The carburisation of the second sample was carried out under pure ethylene and to a higher carburisation degree – in order to obtain a mass increase equal to  $0.154 \text{ g C/g Fe}$  (TG 2). The same procedure was repeated to obtain the third sample, containing  $0.328 \text{ g C/g Fe}$  (TG 3).

The XRD spectra of the samples after carburisation are shown in Figure 2. Under the conditions of the experiments, no  $\alpha\text{-Fe}$  peaks were detected for any of the samples. The non-marked peaks in the spectra correspond to the  $\text{Fe}_3\text{C}$  phase. The mean crystallite size of the obtained iron carbide, calculated using the Scherrer equation, was found to be in the range of 40–46 nm.

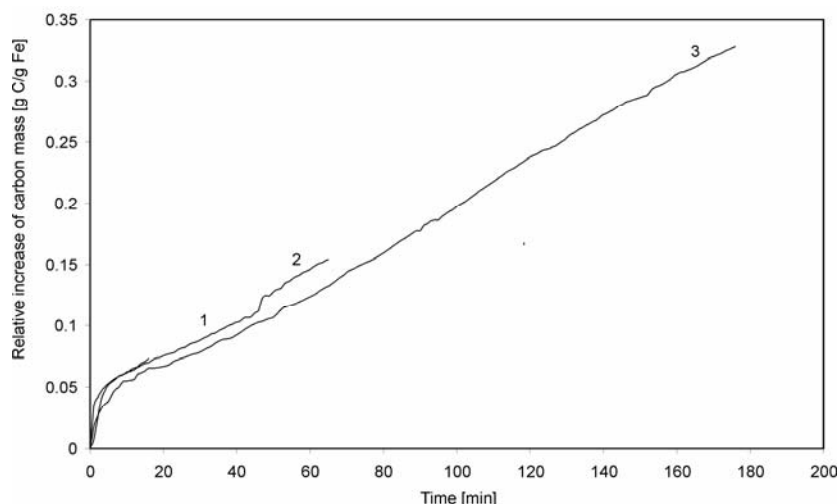


Fig. 1. TG curves of the carburisation process of nanocrystalline iron at 400 °C:  
 1 – carburisation under an ethylene–hydrogen mixture (1:3) up to 0,072 g C/g Fe,  
 2 – carburisation under pure ethylene up to 0,154 g C/g Fe,  
 3 – carburisation under pure ethylene up to 0,328 g C/g Fe

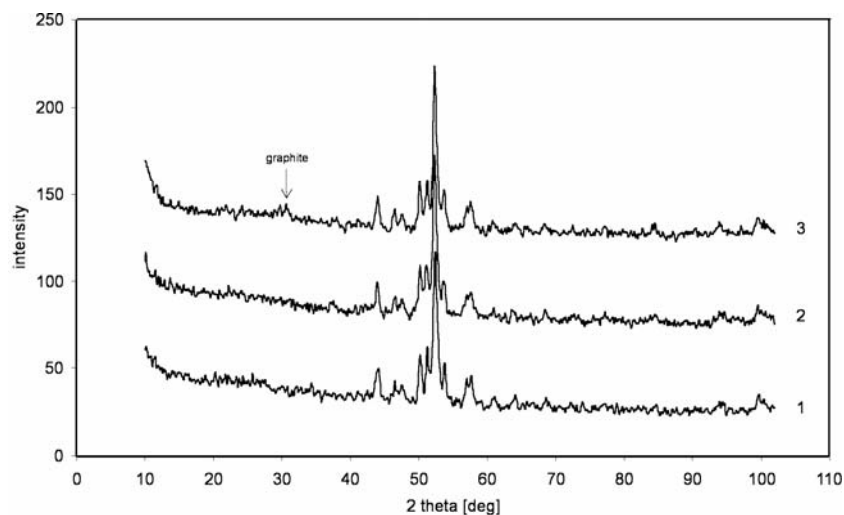


Fig. 2. XRD spectra of samples I–III after carburisation

The intensity of  $\text{Fe}_3\text{C}$  peaks in all the investigated samples is approximately the same. The amount of carbon in the samples is different, however, and samples II and III contain free carbon. It is difficult to distinguish the peak of graphite at  $2\theta = 30^\circ$  in the diffraction pattern No. 2. This peak can be observed only in the case of the most carburised sample (diffraction pattern No. 3). Even in this case the peak of graphite is weak and wide, indicating the formation of very fine crystallites of graphite.

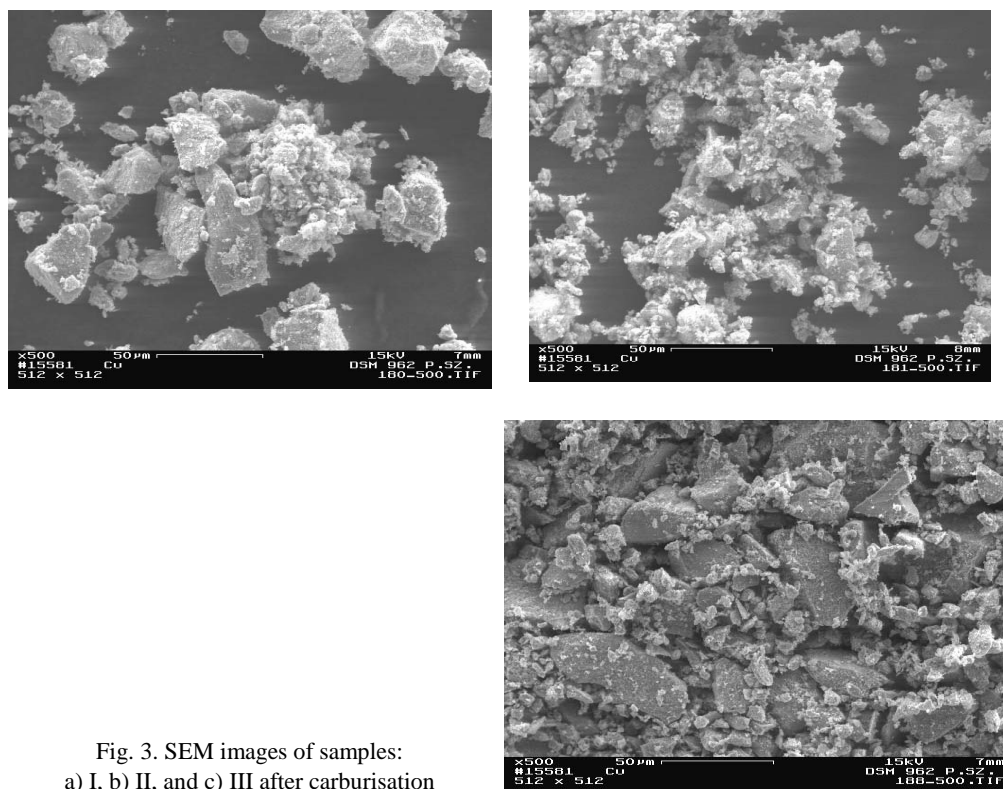


Fig. 3. SEM images of samples:  
a) I, b) II, and c) III after carburisation

SEM images of the samples are presented in Figure 3. The resolution does not allow final conclusions to be drawn about the form of carbon deposits on the sample surface. There are insignificant differences between the SEM images of the samples, which is not astonishing taking into account that the SEM technique concerns only the morphology of the surfaces of grains and that carbon deposits form mainly inside the porous grain. The initial material is very porous (about 50%) and each grain of the sample is composed of fine iron crystallites 17 nm in diameter. After the reaction, carbon deposits form on the surface of each iron crystallite (transformed into iron carbide crystallite as a result of the reaction).

The strongly magnetic materials  $\text{Fe}_3\text{C}$  and  $\text{Fe}_3\text{C}/\text{C}$  were forced into the rigid state by a special procedure involving a non-magnetic material in a quartz tube. Before FMR measurements were performed, the samples had been magnetized several times in a steady magnetic field up to 1.6 T. This process allowed the same FMR spectra to be recorded, independent of whether the magnetic field is swept with increasing or decreasing values. This is especially important for the low-magnetic-field part of the FMR spectrum, where the line position displays a large shift (shifts to higher magnetic fields in the case of a sweep with increasing values). Figure 4 presents the FMR spectra for the investigated samples for an increasing and decreasing sweep of the applied magnetic field. Very intense and strongly asymmetric absorption lines, shifted

in the direction of low magnetic fields, were obtained. It was observed that for samples with an increased carbon concentration the intensity of the FMR spectrum decreased, while the position of the resonance line shifted to higher magnetic fields.

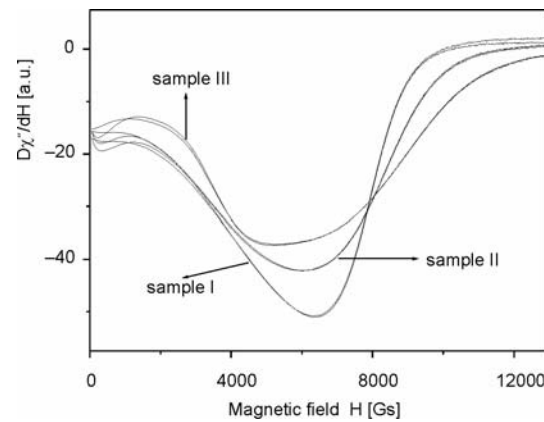


Fig. 4. The FMR spectra of iron carbide with different carbon concentrations at room temperature. Each spectrum is swept toward increasing and decreasing values of the applied magnetic field

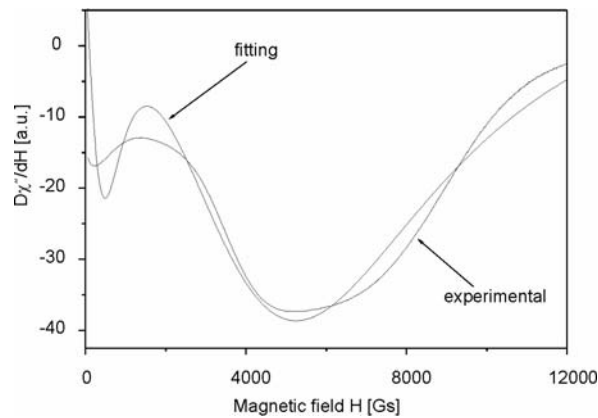


Fig. 5 The fitted and experimental FMR spectra of sample I

As a first approach, a rough fitting of the extended FMR signal was performed using the Lorentzian-type curves, taking into account the absorption at both  $H_r$  and  $-H_r$  magnetic fields, induced by the two oppositely rotating components of the linearly polarised rf field. The FMR spectra for all samples were satisfactory fitted with two Lorentzian curves, having resonance magnetic fields near zero and at higher values (Fig. 5). Table 1 shows the obtained values of the resonance field  $H_r$ , the peak-to-peak linewidth  $\Delta H$ , and integrated intensity  $I_{\text{int}}$  ( $I_{\text{int}} = A\Delta H^2$ , where  $A$  is the signal amplitude). With an increase of the carbon concentration, the resonance field of the main line strongly shifts to higher magnetic fields, while the linewidth and intensity de-

crease. The shift of the resonance field is connected to the strong ferromagnetic interaction between agglomerates. As the carbon concentration increases, the separation between agglomerates increases and the magnetic interaction decreases. The internal field produced by neighbouring magnetic dipoles is averaged due to the spherical symmetry of the environment. The broadening of the FMR line is caused by dipole–dipole interaction, which has the largest influence on the spectra.

Table 1. The values of FMR spectra parameters for the three studied samples of iron carbide with different carbon concentrations

Sample	Resonance field $H_r$ [Gs]	Linewidth $\Delta H_1$ [Gs]	Linewidth $\Delta H_2$ [Gs]	Relative intensity $I_1$ [a. u.]
I	2660(10)	11900(10)	3270(10)	10.9
II	2832(10)	10740(10)	2140(10)	5.9
III	2990(10)	9050(10)	3270(10)	3.9

In conclusion, three samples of iron carbides, with various carbon concentrations, have been prepared. The carbon concentration had a strong influence on the observed FMR spectra of all samples. The ferromagnetic interaction between agglomerates strongly decreases with increasing carbon concentration.

#### Acknowledgements

This work was partially supported by the grant PBZ-KBN-095/TO8/2003.

#### References

- [1] BI X.-X., GANGULY B., HUFFMAN G.P., HUGGINS F.E., ENDO M., EKLUND P.C., *J. Mater. Res.*, 8 (1993), 1666.
- [2] ZHAO X.Q., LIANG Y., ZHU Q., LIU B.X., *J. Appl. Phys.*, 80 (1996), 5857.
- [3] GRIMES C.A., HORN J.L., BUSH G.G., ALLEN J.L., EKLUND P.C., *IEEE Trans. Magn.*, 33 (1997), 3736.
- [4] GRIMES C.A., QIAN D., DICKEY E.C., ALLEN J.L., EKLUND P.C., *J. Appl. Phys.*, 87 (2000), 5642.
- [5] DENES F.S., MANOLACHE S., MA Y.C., SHAMAMIAN V., RAVEL B., PROKES S., *J. Appl. Phys.*, 94 (2003), 3498.
- [6] GOODWIN T.J., YOO S.H., MATTEAZZI P., GROZA J.R., *Nanostruct. Mater.*, 8 (1997), 559.
- [7] YUMOTO H., NAGAMINE Y., NAGAHAMA J., SHIMOTOMAI M., *Vacuum*, 65 (2002), 527.
- [8] PSARRAS G.C., MANOLAKAKI E., TSANGARIS G.M., *Composites A*, 34 (2003), 1187.
- [9] BICKFORD L.R., *Phys. Rev.*, 78 (1950), 449.
- [10] SHARMA V.N., *J. Appl. Phys.*, 36 (1965), 1450.
- [11] GRISCOM D.L., FRIEBELE E. J., SHINN D. B., *J. Appl. Phys.*, 50 (1979), 2402.
- [12] GRISCOM D.L., *IEEE Trans. Magn. MAG*, 17 (1981), 2718.
- [13] GRISCOM D.L., *J. Non-Crystalline Solids*, 67 (1984), 81.
- [14] MALHOTRA V.M., GRAHAM W.R.M., *J. Appl. Phys.*, 57 (1985), 1270.
- [15] SHARMA V.K., WALDNER F., *J. Appl. Phys.*, 48 (1977), 4298.
- [16] DE BIASI R.S., DEVEZAS T.C., *J. Appl. Phys.*, 49 (1978), 2466.

- [17] NARKIEWICZ U., GUSKOS N., ARABCZYK W., TYPEK J., T BODZIONY., KONICKI W., GASIOREK G., KUCHARIEWICZ I., ANAGNOSTAKIS E.A., Carbon, 42 (2004), 1127.
- [18] GUSKOS N., ANAGNOSTAKIS E.A., TYPEK J., BODZIONY T., NARKIEWICZ U., Mol. Phys. Rep., 39 (2004), 58.
- [19] GUSKOS N., TYPEK J., NARKIEWICZ U., MARYNIAK M., AIDINIS K., Rev. Adv. Mater. Sci., 8 (2004), 10.
- [20] BODZIONY T., GUSKOS N., TYPEK J., ROSLANIEC Z., NARKIEWICZ U., MARYNIAK M., Rev. Adv. Mater. Sci., 8 (2004), 86.
- [21] GUSKOS N., ANAGNOSTAKIS E.A., LIKODIMOS V., TYPEK J., BODZIONY T., NARKIEWICZ U., J. Appl.Phys., 97 (2005), 024304.

*Received 2 December 2004*

*Revised 25 March 2005*